International Symposium COMODIA 90: 249-254(1990)

Numerical Simulation of Flow and Combustion of Transient Sprays

T.Takagi, C.Y.Fang, T.Kamimoto* and T.Okamoto

Department of Mechanical Engineering
Osaka University
Suita, Osaka 565
Japan
* *Tokyo Institute of Technology*

ABSTRACT

Numerical simulations of transient sprays were made based on an Eulerian gas and a Lagrangian drop formulation incorporated with chemical reactions for the gas and for soot. Computed profiles of axial and radial velocity, species and soot concentration, gas temperature, local or total heat release rate versus time are presented to understand the overall and the internal structure of the combusting spray. Some of the computed results are compared with experiments taken in a rapid compression machine. The results indicate the following. (1) The computations predict the ignition delay, the transient configuration of the spray flame and drop penetration distance reasonably well. (2) The drops evaporate in the early stage of the spray combustion and the drop penetration distance is predicted well by taking account of the secondary breakup of the drops in the evaporating sprays. The secondary breakup is liable to occur at high pressure and high temperature atmosphere. (3) Ignition occurs at a hot spot in the off-axis region followed by the rapid spread of the combustion and the fast release of heat. (4) A flame front is formed downstream from the nozzle exit. Near the flame front, the local heat release rate is very intense where premixed combustion occurs. Gaseous turbulent diffusion dominates combustion of the fuel in the core of spray.

INTRODUCTION

Spray combustion includes complex processes such as drop formation, collision, coalescence secondary breakup, evaporation and interaction with turbulence as reviewed by Faith(1), Lefebre(2) as well as turbulent mixing and chemical reactions. Experimental(3) and numerical (4) studies of non-transient spray combustion have contributed to the understanding of spray combustion processes and to elucidate the internal structure of spray flames.

As far as transient spray combustion as encountered in Diesel engines, experimental studies were conducted in rapid compression machine (5), (6) to get information about configuration and internal structure, but the measured quantities are limited. Numerical methods have been developed to simulate transient sprays with and without evaporation (7). No study seems to have been published to compare computed and measured results of evaporating and combusting transient sprays.

In this work, evaporation, ignition and combustion were computed and comparisons were made with measurements taken in a rapid compression machine operated at high pressure and high temperature atmosphere in order to elucidate the process and the internal structure of the transient combusting spray.

FUNDAMENTAL EQUATIONS

The fundamental equations are the transient Eulerian equations for the gas in cylindrical coordinates and the Lagrangian equations for drops (7). The equations include [1] the conservation equations of mass, momentum and energy for the gas, [2] the conservation equations for gas species and soot, [3] the k-ε transport equations for turbulent kinetic energy and rate of turbulent energy dissipation [4]the exchange rate equations of heat, mass and momentum between gas and drops (7), [5] the state equation of gas and [6] reaction models for gas species (8), (9), (10) and soot (10), (11), (12). The equations are given in the references.

Other auxiliary equations are [1] the equation to determine the drop collision frequency and the equation to determine the coalescence probability of drops (7), [2] the equation to determine the exit Sauter mean diameter of the drops and the injection angle (13), [3] the equation to determine the secondary breakup of drops.

All equations are solved numerically in fully coupled form.

THE CONDITIONS AND THE METHOD OF COMPUTATIONS

The computed sprays are the axisymmetric transient ones that are formed when liquid fuel (tridecane) is injected from a single hole nozzle into stagnant, high-pressure and high-temperature atmosphere.

An axisymmetric cylindrical volume is considered as the computation domain. The origin

of the axisymmetric coordinate system is located at the center of the nozzle exit. The axial coordinate x is adjusted to the spray axis and the coordinate y is in the radial direction.

The domain is divided into 44 cells in the x direction and 21 in the y direction. The cell size is not uniform and is smaller near the nozzle and near the axis.

The initial and boundary conditions are as follows. The gas is stagnant initially. All dependent variables of the gas properties such as gas temperature, pressure, kinetic energy of turbulence, and its dissipation rate are assumed to be uniform initially.

The downstream and side boundaries of the domain are treated as open boundaries where the radial and axial derivatives of the variables are set equal zero. The radial gradients are nil also across the axis. The upstream boundary is treated as a solid wall with no slip for the velocity and zero normal gradients for scalar quantities. Drops are injected from the hole of the nozzle with injection velocity Vinj. The injection angle of the drop is selected in a random way between 0 - θ. The maximum injection angle θ is estimated from the injection velocity and the surrounding gas density (13). The liquid core at the nozzle exit is neglected. The drop size distribution at the nozzle exit is considered.

The computed condition corresponds to one of experiments which were conducted with a rapid compression machine (5). Liquid injection pressure Pinj is 30 Mpa. The pressure and temperature of the ambient air is 3 Mpa and 900 K, respectively. The nozzle diameter is 0.16 mm. The injection velocity of the spray, Vinj is 185 m/s which is estimated from the difference between the injection pressure and the ambient pressure. The drop mass-averaged radius at the exit of the nozzle is given to be 1.0 μm which is estimated from the injection velocity, gas density and surface tension (13). Liquid fuel injection lasts 4 ms at a constant flow rate.

RESULTS AND DISCUSSIONS

Prior to computations for spray combustion, computations were made for non-evaporating and evaporating sprays. The computed condition is the same with that mentioned above except that the atmosphere is nitrogen gas instead of air and for non-evaporating spray, the atmospheric temperature is 300 K.

Figure 1(a) and (b) show penetration distance of droplets X versus time t for non-evaporating and evaporating sprays, respectively. Plots in

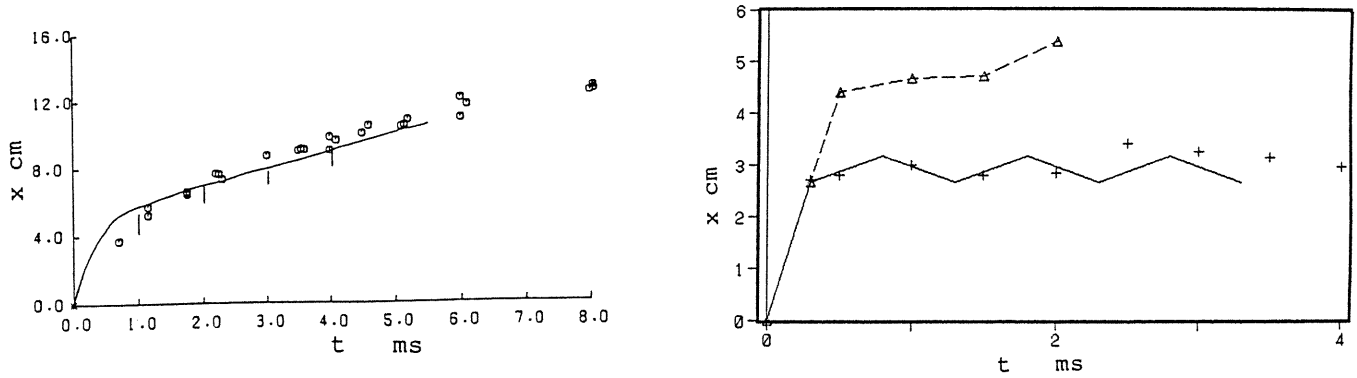

(a) non-evaporating spray

(b) evaporatin spray

Fig.1 Penetration distance

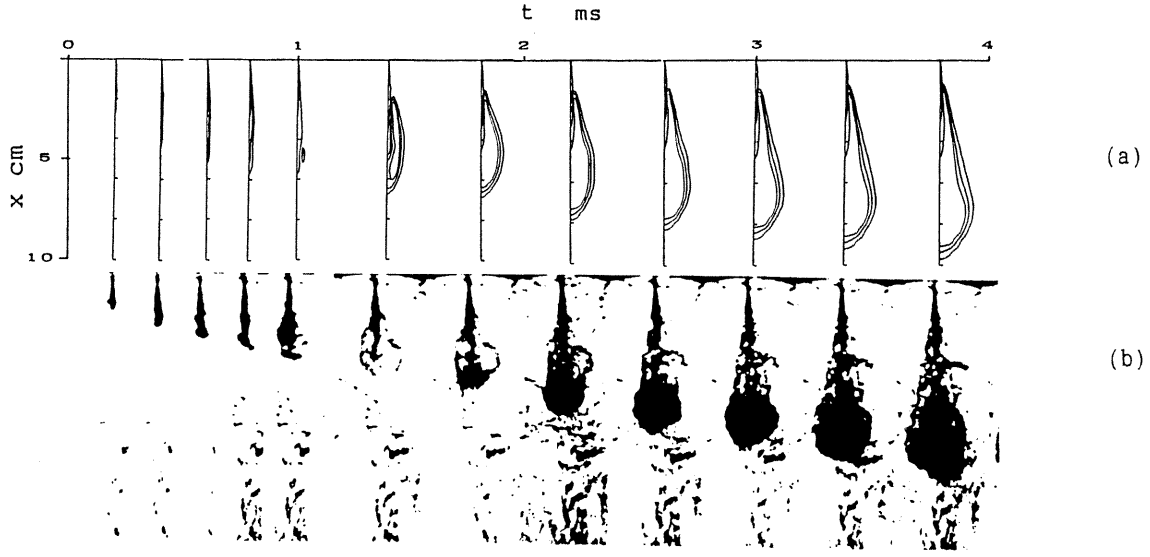

Fig.2 Comparison of the computed equi-temperature contours (a) and schliren photographs (b).

Fig.1(a) are measured results(5) and the line is the computed one. The penetration distance of the non-evaporating spray extends with respect to time and the computation predicts the experimental results well. The solid line in Fig.1(b) is the measured one(5) and the plots (cross) are the computed ones taking account of the secondary breakup of the droplets. When taking account of the secondary breakup, drop is assumed to break up into two equal drops when the Weber number We (= ρ_g(V-U)^{2}r/σ) reaches a critical number Wec where ρ_g = gas density, V-U is relative velocity of drop and gas, σ = surface tension, r = drop radius. The critical number is assumed to be 20 which is estimated from Lefebre(2). The plots (triangle connected by the broken line) is the computed results without considering the secondary breakup.

Figure 1(b) shows that the penetration distance increases with respect to time at early time, but the distance is kept nearly constant after x reaching about 3 cm in experiments. The nearly constant penetration with respect to time is due to the evaporation of the drops. The computation taking account of the secondary breakup predicts well the experimental drop penetration. The computations without considering the secondary breakup estimate longer penetration distance. The socondary breakup is liable to occur under high pressure and high temperature atmosphere.

The results of computations for the combusting spray are presented below.

Figure 2(a) shows the computed isotherms at different times during injection. Fig.2(b) shows the corresponding experimental Schlieren photographs(5). The Schlieren photographs indicate that ignition occurs at about t = 1 ms. The calculated isotherms indicate that the temperature rise initiates at about t = 1 ms. The location of the ignition (rapid temperature rise) is off-axis and just upstream of the tip of the spray. After ignition, the radial extent of the spray increases due to the expansion of the gas. The computed configuration of the spray and the penetration distance correspond fairly well to the measured ones.

Figure 3(a) and (b) show the computed temperature profiles and local heat release rate q in time series near the ignition, respectively. Time t after the ignition corresponds for both figures. The minimum temperature is observed near the nozzle exit and on the spray axis and the temperature is far below the ambient temperature because of the heat absorption by the drops. Generally, the temperature is higher at off-axis region. At about t = 1.0 ms, hot spot above 1000 K is formed. The temperature at the hot spot increases rapidly and the high temperature region extends surrounding the spray axis with lapse of time. This combustion is supposed to be a premixed combustion combined with the ignition and flame propagation.

Local heat release rate per unit volume due to chemical reactions as shown in Fig.3(b) indicates the following. [1] At t=1.05, 1.2 and 1.4 ms just after the ignition, the local heat relrease rate is large where temperature is high. The vapour premixed with air prior to the ignition seems to burn. [2] At t=3.7 ms, the heat release rate is very large near the flame front nearly at x = 1.5 cm. The flame front is denoted by the front of the temperature profiles in Fig.3(a). The high heat release rate near the flame front is caused by the premixed type combustion where the fuel vapor evaporated in the upstream of the flame front is premixed with the surrounding air prior to the combustion. In the downstream, the heat release rate is observed at the circumferential region and near the tip of the flame where the the heat release rate is not intense but the region of the heat release extends widely to the off-axis region. The heat release at the circumferential region is supposed to be caused by the turbulent diffusion combustion.

Figure 4 shows computed radial profiles of axial velocity of gas (solid lines) and mass averaged velocity of droplets (dots) versus radial distance y at two cross sections (axial distance from the nozzle exit x is 1.7 and 4.5 cm) at three different times. At x=1.7cm, the gas velocity profile does not change much which means that steady condition is reached near the nozzle exit. Drop velocity is higher than the gas velocity. At x=4.5 cm, gas velocity increases with lapse of time. No drop is found there.

Figure 5 shows computed radial profiles of radial velocity component at the same place and time with those of Fig.4. At x=1.7 cm, negative radial velocity is observed which indicates the entrainment of the surrounding air into the spray. Positive radial velocity at x=4.5 cm at t=1.0 and 1.2 ms indicates outward flow pushed out by the spray. Significantly large positive velocity at X=4.5 cm and t=1.2 ms is induced by the expansion due to combustion. At x=4.5 cm, at t=3.7 ms, negative velocity is found because the flow induced by the spray extends far downstream and entrainment is induced even at the position of x=4.5cm.

Figure 6 shows the heat release rate Q which is the net total heat release rate in the whole flow field. Up to t = 0.8 ms the heat release rate is negative due to the heat absorption by the drops. Near at t = 1.0 ms heat release rate increases promptly to reach maximum which is much larger than that estimated by the fuel supply rate per time. This indicates that the accumulated fuel vapour evaporated and premixed with the surrounding air prior to the ignition burns rapidly after the ignition. This corresponds to the rapid spread of the hot region (spot) during the ignition observed in Fig.3. The heat release rate decreases to reach minimum value near at t = 2 - 2.5 ms and then increases even if the fuel supply rate is kept constant. The increase of the heat release rate after reaching the minimum value may be caused by the enhanced evaporation of the fuel droplets by the high temperature gas after the flame spread. These characteristic tendency of the heat release rate corresponds to that observed in Diesel engines and rapid compression machine (6).

Figure 7 shows the schematic picture based on the calculation at time t=3.7 ms when considerable time has passed after ignition. Small dots indicate the positions of the fuel drops. The drops disappear nearly up to x = 3 cm due to the evaporation. The existence of the drops is limited to local region near the nozzle exit. The equi-concentration line of the evaporated fuel vapor is indicated by the dotted lines. High concentration of the vapor is observed at x = 2 - 4 cm near the

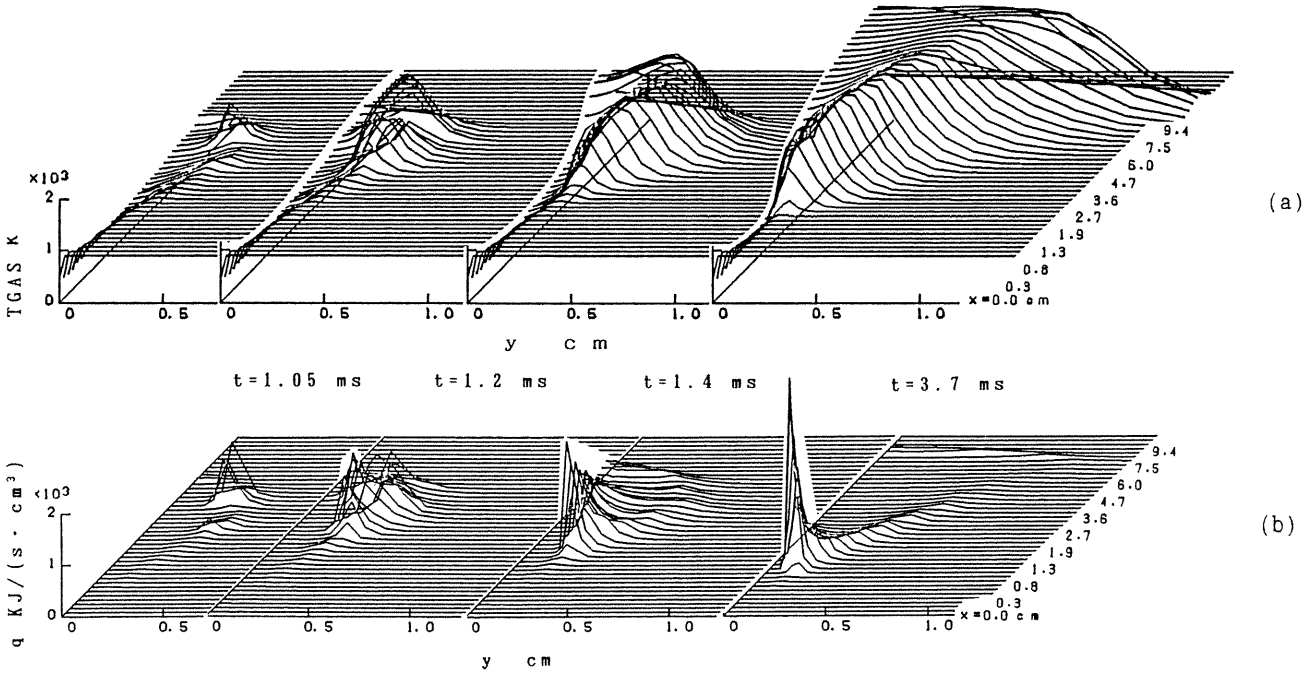

Fig.3 Profiles of temperature (a) and local heat release rate (b).

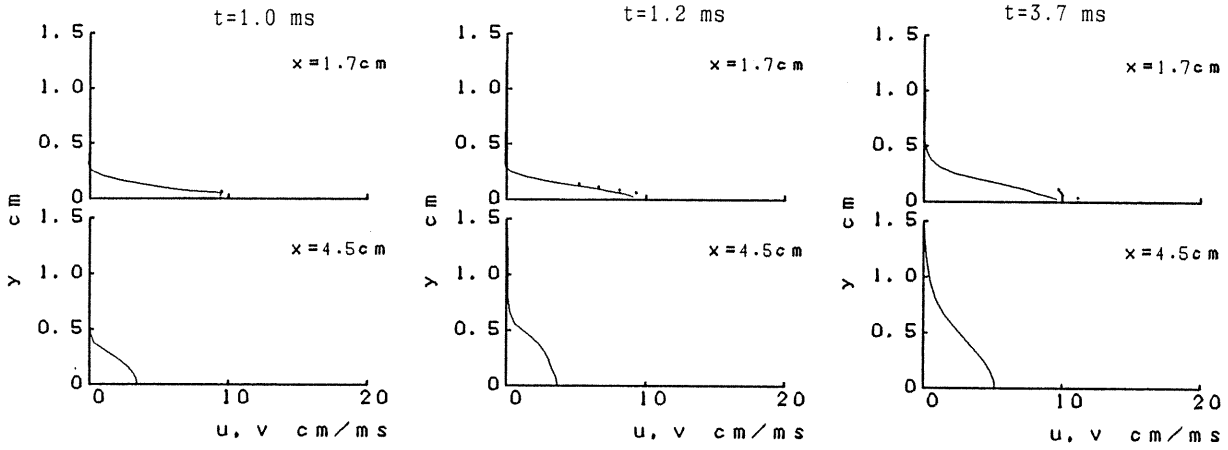

Fig.4 Radial profiles of axial velocity of gas u_x and drop v

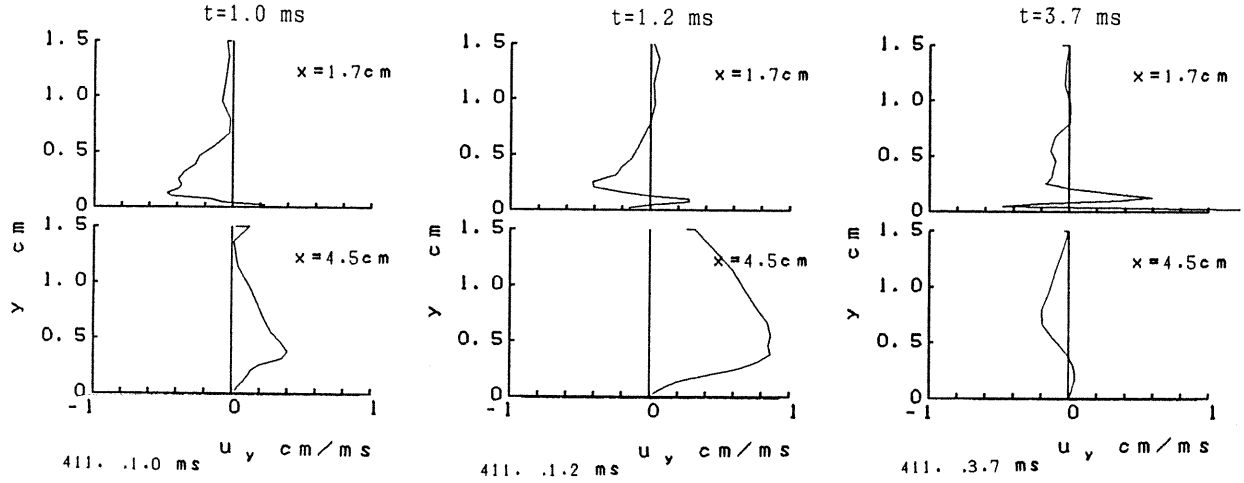

Fig.5 Radial profiles of radial velocity of gas u_y.

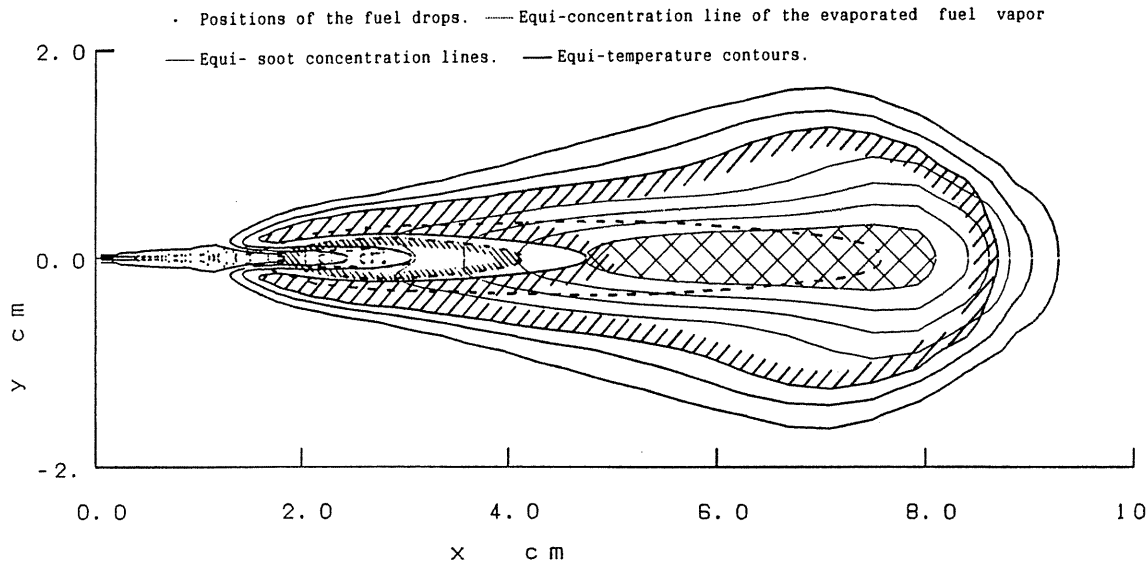

Fig.7 Schematic picture of the spray flame (t = 3.7 ms).

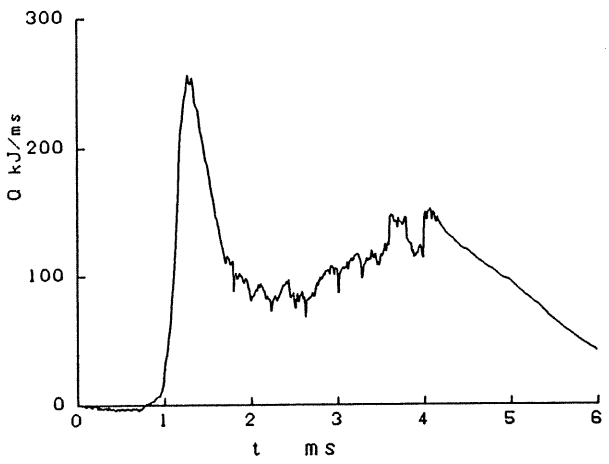

Fig.6 Net heat release rate versus time.

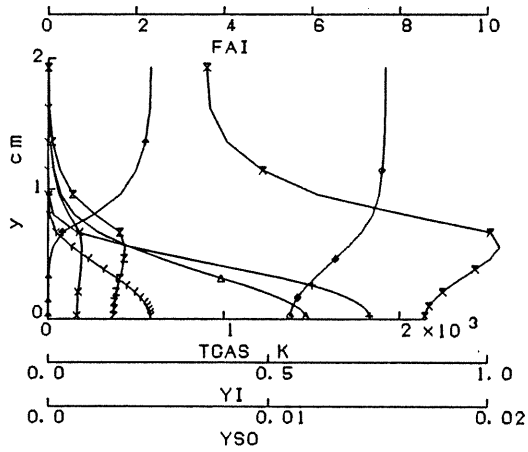

(x = 4.4 cm, t = 3.7 ms).

Fig.9 Radial profiles of various properties

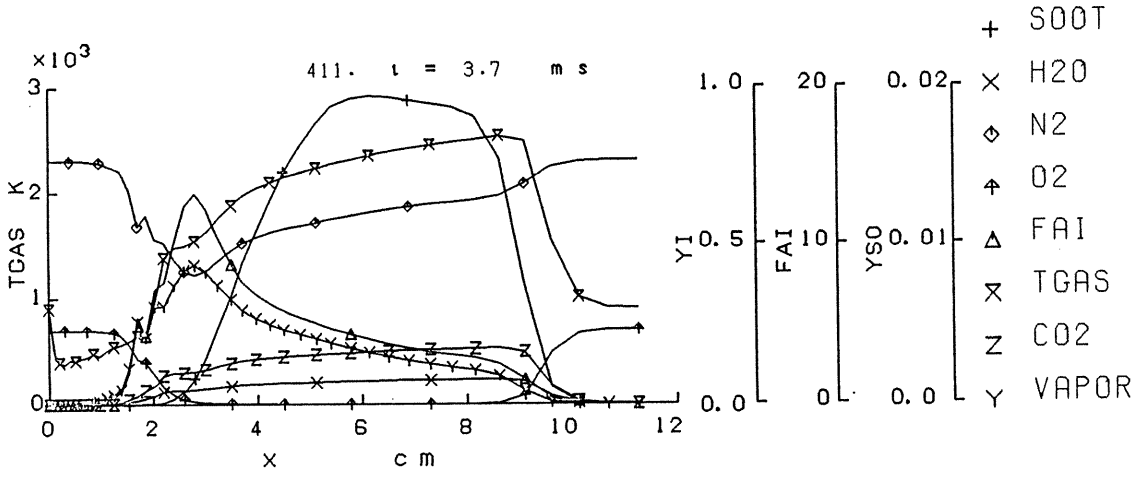

Fig.8 Axial profiles of various properties (t = 3.7 ms).

central axis (indicated by the dashed lines). The fuel vapor region extends up to x = 8 cm. The gaseous turbulent diffusion combustion seems to dominate in the large portion of the flame as postulated in the non-transient spray combustion (3). Equi-temperature contours are indicated by thick solid lines. Low temperature region corresponds to the drop-existing region and high-vapor-concentration region near the nozzle exit. The high temperature region is observed at the circumferential part at x = 2 - 5 cm and at the central part in the downstream (indicated by the dashed lines). The equi-soot concentration lines are indicated by the thin solid lines. The high soot concentration (indicated by mesh) is observed in the downstream region indicated by the dashed lines. This corresponds to the experimental fact because the Schlieren photographs of Fig.2 indicates the soot existence by the dark shadow near the downstream region.

In Figs.8 and 9, computed axial and radial profiles of gas temperature (TGAS), species gas concentration (YI), soot concentration (mass fraction), local equivalence ratio (FAI) are shown at t = 3.7 ms. Plots do not denote the calculation grids but indicate which line denotes which quantity. The figures support quantitatively what were pointed out in Fig.7.

Figure 8 indicates the following. [1] Gas temperature is maximum near the tip of x = 8.5 cm where equivalence ratio is nearly unity and it decreases sharply in the downstream. [2] Fuel vapor concentration and the equivalence ratio become very high at x = 2 - 3 cm. Fuel rich condition is maintained on the axis near up to x = 8 cm. [3] Soot concentration becomes maximum at x = near 7 cm whose location is downstream not far from the flame tip. The soot formation rate estimated in the present calculation becomes large in the upstream region but the convection of the soot significantly shifts the concentration peak downstream.

Figure 9 indicates that profiles of the fuel vapor, O_2, H_2O, CO_2 and temperature are similar to those of the typical turbulent gas diffusion flame (14). That is to say, the fuel vapor and oxygen concentration is high at the central part and circumferential part, respectively. CO_2 and H_2O concentration and temperature are high at the boundary where fuel vapor and oxygen meet and equivalence ratio is near unity.

SUMMARY

Numerical simulations on the transient sprays were made based on the Eulerian gas and Lagrangian drop formulations coupled with chemical reactions of gases and soot. Some of the comuputed results were compared with the experiments conducted using a rapid compression machine. The results obtained are as follows.
(1) The computations predict the ignition delay, the transient configuration of the spray flame and the drop penetration distance reasonably well.
(2) The drops evaporate in the early stage of the spray combustion. The drop penetration distance were predicted well by taking account of the secondary breakup of the drops. The secondary breakup is liable to occur at a high pressure and high temperature atmosphere.
(3) Ignition is initiated by the hot spot at the off-axis region followed by the rapid spread of combustion region which induces intense heat release rate just after the ignition.
(4) Flame front is formed downstream from the nozzle exit. Near the flame front, the local heat release rate is very intense where premixed combustion occurs. Gaseous turbulent diffusion combustion dominates in the downstream.

ACKNOWLEDGEMENT

This work is supported by the Grant-in-Aid for Scientific Research on Priority Areas, the Ministry of Education, Science and Culture of Japan.

REFERENCE

(1)Faith, G.M.(1987). Mixing Transport and Combustion in Sprays. Pro. Energy Combust. Sci. 13, 295.
(2)Lefebre, A.H.(1989). Atomization and Sprays, Hemisphere Publising Corporation, New York.
(3)Onuma, Y. and Ogasawara, M.(1974). Studies on the Structure of a Spray Combustion Flame. Fifteenth Symposium (International) on Combustion, p.453, The Combustion Institute.
(4)Wild, P.N., Boisan, F. and Swithenbank, J.(1988). Spray Combustion Modeling. J. Inst. Energy, March, 27.
(5)Yokota, H., Kamimoto, T. and Kobayashi, H. (1988). A Study of Diesel Spray and Flame by an Image Processing Technique (1st Rep.). Bulletin of JSME, 54, 741.
(6)Yokota, H., Kamimoto, T., Kobayashi, H. and Tujimura, K.(1990). A Study of Diesel Spray and Flame by an Image Processing Technique Eighth Joint Symposium (Japan) on Internal Combustion Engines, In press, Japan Society of Mechanical Engineers.
(7)O'rourke, P. J.(1981). Collective Drop Effects on Liquid Spray. Ph. D. Thesis, Princeton University.
(8)Westbrook, C. K. and Dryer, F. L.(1981). Simplified Reaction Mechanisms for the Oxidation of Hydrocarbon. Combust. Scien. Techno., 27, 31.
(9)Aggarwal, S. K.(1987). Chemical-Kinetics Modeling for the Ignition of Idealized Sprays. Combust. Flame 69, 291.
(10)Magnussen, B. F. and Hjertager, B. H.(1977). On Mathematical Modeling of Turbulent Combustion With Special Emphasis on Soot Formation and Combustion. Sixteenth Symposium (International) on Combustion, p.719, The Combustion Institute.
(11)Lee, K. B., Thring, M. W. and Beer, J. M.(1962). On The Rate of Soot In a Laminar Soot Flame. Combust. Flame, 6,137.
(12)Abbas, A. S. and Lockwood, F. C.(1985). Prediction of Soot Concentrations in Turbulent Diffusion Flames. J. Inst. Energy., September, 112.
(13)Kuo, T. W. and Bracco, F. V.(1982). Computations of Drops Sizes in Pulsating Sprays and of Liquid-Core Length in Vaporizing Sprays. SAE paper, 820133.
(14)Takagi, T., Okamoto, T.(1986). Studies on Turbulent Diffusion on Flames (3rd Report). Bulletin of JSME., 52, 1540.